J Therm Anal Calorim (2012) 108:965–970
DOI 10.1007/s10973-011-2149-6

Investigations on NH_4VO_3 thermal decomposition in dry air

A. Biedunkiewicz · U. Gabriel · P. Figiel · M. Sabara

ICVMTT2011 Conference Special Chapter

Abstract The results of investigations on thermal decomposition of NH_4VO_3 in dry air have been presented. TG–DSC measurements were carried out under non-isothermal conditions at linear change of samples temperature in time and under isothermal conditions. Characterization of the products structure was performed by XRD method. MS method was used to determine evolved gaseous products. The decomposition of NH_4VO_3 was described by the following equation:

$$6NH_4VO_3 \rightarrow (NH_4)_3V_6O_{16} \rightarrow (NH_4)_2V_6O_{16} \rightarrow V_2O_5.$$

Keywords Ammonium metavanadate · Thermal decomposition · TG–DSC method

List of symbols

α	Conversion degree
β	Heating rate/K/min
m_0	Initial sample mass for the stage/mg
m	Current sample mass for the stage/mg
m_k	Final sample mass after for the stage/mg
t	Time/min
T	Temperature/K
T_o	Initial temperature of the stage/K
T_m	Temperature corresponding to peak maximum/K
TG_u	Normalized TG

A. Biedunkiewicz (✉) · U. Gabriel · P. Figiel · M. Sabara
Institute of Materials Science and Engineering, West Pomeranian University of Technology in Szczecin, Av. Piastow 19, Szczecin, Poland
e-mail: anna.biedunkiewicz@zut.edu.pl

Introduction

Carbides, carbonitrides, and vanadium oxides are known ceramic materials [1]. Composites containing vanadium carbides or carbonitrides are also manufactured [2–4]. NH_4VO_3 could be used in these processes as a precursor. In the low temperature stage V_2O_5 is obtained, and in the high-temperature stage, during carbothermal reduction of V_2O_5, vanadium carbide is obtained, during carbothermal reduction and nitriding vanadium carbonitride, and during the carbothermal reduction with the presence of boron, vanadium boride is received. It should be added that V_2O_5 is also used during preparation of catalysts for VOCs total oxidation processes [5] and for catalytic selective reduction of NO_x [6]. The activity of these catalysts depends on size and morphology of V_2O_5 particles. During the preparation of nanometric V_2O_5 catalysts NH_4VO_3 can be used.

The transitions with participation of solid reagents usually proceed in many stages. Each step should be treated as an independent process. The courses of heterophase non-catalytic reactions are usually investigated with use of thermogravimetric methods. Our measurements were performed under isothermal and non-isothermal conditions on standard TG–DSC apparatus [7–9].

Experimental

NH_4VO_3 from Fluka was used as a substrate. Decomposition was performed in dry air (Messer, Germany) containing 20.5 vol% O_2, rest N_2. Impurities occurred in amounts: $H_2O < 10$ vpm, $CO_2 < 0.5$ vpm, $NO_x < 0.1$ vpm, hydrocarbons < 0.1 vpm. Thermogravimetric measurements were carried out on TG–DSC Q600 (TA Instruments) apparatus. Gaseous products of proceeding transitions were identified by

mass spectrometry method. Pfeifer Vacuum ThermoStar GDS 301 apparatus was used. Solid products were identified by XRD method. X'Pert Pro apparatus from PANalytical with a copper X-ray tube with current voltage 35 kV and intensity 40 mA was used. Spectra processing and analysis was performed using X'Pert HighScore 1.0 software with incorporated ICDD spectra library.

Results

Temperature, TG_u, DTG, HF functions, and mass spectra of volatile products have been registered in time. The measurements were carried out at sample heating rates of 2, 3, 4, 5, 6, 7, 8, and 10 K/min. Masses of the samples were in the order of 20 mg. The process has been divided into stages and dependency of conversion degree on temperature has been calculated for selected stages.

In Fig. 1 there are presented jointly TG_u, DTG, and HF dependencies on temperature obtained at sample heating rate of 2 K/min.

It is visible that decomposition of NH_4VO_3 proceeded in three, endothermic stages. In Fig. 2 there are shown TG_u function and mass spectra curves of NH_3 ($m/e = 17$); H_2O ($m/e = 18$); NO ($m/e = 30$); N_2O ($m/e = 44$) depending on time. In the system no NO_2 occurred.

Elimination of NH_3 proceeded in all stages (Fig. 2). There should be added that NO and N_2O were formed as a result of oxidation of evolved NH_3. On the basis of TG plot mass losses of the sample in stages have been calculated. The total sample mass loss in this measurement equaled 22.18 wt%. Theoretical mass loss for decomposition of NH_4VO_3 into V_2O_5, equals 22.29 wt%. The mass loss in stage I equaled 11.48 wt%, in stage II 4.04 wt% (with reference to the initial sample mass) and in stage III 6.66 wt%.

In Table 1 there are listed sample mass losses in carried out measurement series.

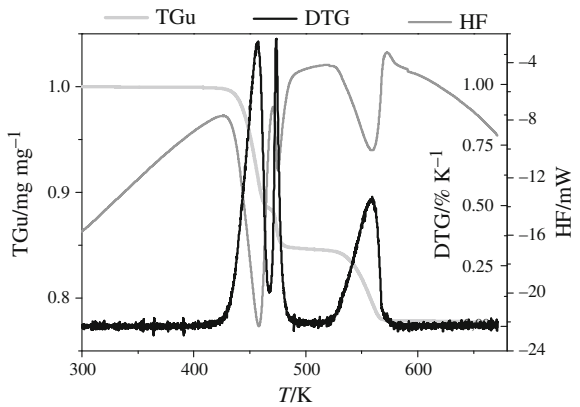

Fig. 1 TG_u, DTG, and HF functions in temperature. Decomposition of NH_4VO_3 in dry air

On the basis of mass balance the course of the process is described in the following way

$$6NH_4VO_3 \rightarrow (NH_4)_3V_6O_{16} \rightarrow (NH_4)_2V_6O_{16} \rightarrow 3V_2O_5 \quad (1)$$

Intermediate products were obtained carrying out the isothermal measurements in temperature ranges corresponding to the stages. For the control the final product was obtained in the same way.

In Fig. 3 TG_u functions in temperature registered during the measurements are presented.

The straight segments correspond to the isothermal conditions. The samples were heated isothermally until the stable mass has been reached (about 30 min).

On the basis of XRD investigation the product of the third stage was attributed to V_2O_5 (ICDD card 85-0601), and second to $(NH_4)_2V_6O_{16}$ (ICDD card 79-205). The assumption that the product of the first stage corresponds to $(NH_4)_3V_6O_{16}$ was made basing on the mass balance (there is no pattern for it in ICDD directory).

Influence of samples heating rate for course of reaction

The influence of samples heating rate on the course of reaction was considered on the basis of TG, DTG, and HF

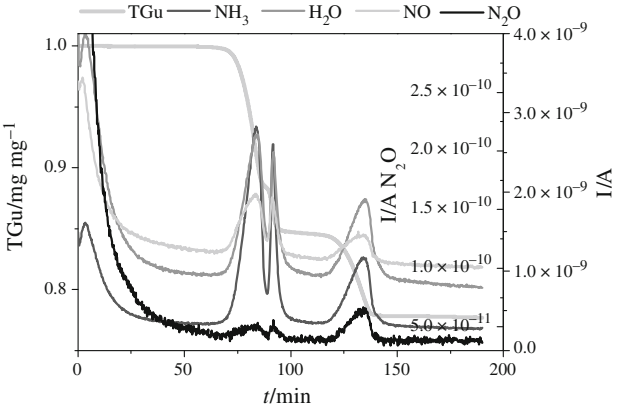

Fig. 2 TG_u and mass spectra of volatile products depending on time. Decomposition of NH_4VO_3 in dry air

Table 1 Sample mass losses in stages

β/K/min	Sample mass loss/wt%			
	I	II	III	Total
2	11.48	4.04	6.66	22.18
2	11.52	3.87	6.77	22.16
5	11.29	4.13	7.14	22.56
7	11.37	3.98	6.98	22.24
10	11.55	3.98	6.91	22.44

Decomposition of NH_4VO_3 in dry air

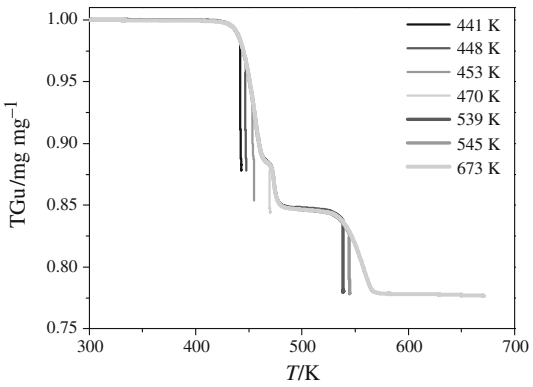

Fig. 3 TG_u functions in temperature. Decomposition of NH_4VO_3 in dry air

function plots and conversion rates determined for all the stages on the basis of TG function.

There should be added that $\alpha(T)$ dependencies for the stages form the basis of process kinetics [10–15].

In work [16] the methods recommended by ICTAC have been presented. While carrying out the measurements the fulfillment of these recommendations was intended. There should be mentioned that decomposition of NH_4VO_3 was investigated earlier [17].

Analysis of TGu, DTG, and HF plots

To facilitate the analysis of the measurement results TGu, DTG, and HF function plots are presented in separated figures. In Fig. 4 TG_u function in temperature is presented. The single curve is formed of about twenty-thousand points.

During the heating of the sample up to 400 °C the decomposition of NH_4VO_3 was completed (TG_u plots end at the same level corresponding to V_2O_5). At the higher sample heating rates passage to this level in not monotonic. This is

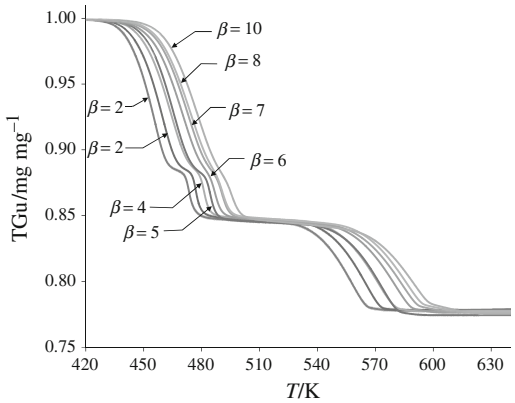

Fig. 4 Plot of TG_u functions in temperature. Decomposition of NH_4VO_3 in dry air

connected with oxidation of V_2O_{5-x} formed earlier (e.g., for $\beta = 6$ K/min; $x = 0.02$). At the higher sample heating rates the stages I and II are overlapped to a larger extent.

In Fig. 5 the plots of DTG functions in temperature are presented.

Along with the increase of sample heating rates the DTG function plots are shifted into the higher temperature range. It is also visible that at the higher sample heating rates stages I and II are overlapped to a larger extent, and the final segments of plots, corresponding to the stage III, are not monotonic. As mentioned before, this was attributed to the oxidation of formed earlier V_2O_{5-x} to V_2O_5.

The T_m temperatures corresponding to peaks of DTG and HF function plots (necessary for Kissinger's method) have been determined.

The results are listed in Tables 2 and 3, respectively.

In Fig. 6 the HF function in temperature has been presented for selected example values of β.

It is visible from the course of HF plots that in the case there are three endothermic stages referred to the NH_4VO_3 decomposition. The HF plots end with the exothermic

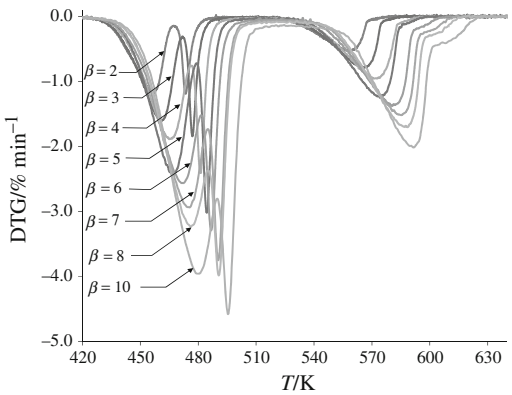

Fig. 5 Plots of DTG function in temperature. Decomposition of NH_4VO_3 in dry air

Table 2 List of T_m temperatures of DTG function peaks for the stages

β/K/min	T_m/°C for DTG		
	Stage I	Stage II	Stage III
2	184.33	200.47	286.13
3	187.41	204.01	292.29
4	191.97	208.23	297.88
5	194.14	211.46	301.15
6	198.39	213.70	307.30
7	202.53	217.30	312.10
8	203.05	217.65	315.61
10	207.35	222.41	318.74

Decomposition of NH_4VO_3 in dry air

Table 3 List of T_m temperatures of HF function peaks for the stages

β/K/min	T_m/°C for HF		
	Stage I	Stage II	Stage III
2	184.88	201.95	285.74
3	189.69	205.69	293.46
4	195.17	209.91	300.25
5	196.64	213.35	302.60
6	203.35	215.26	310.13
7	205.75	218.24	313.38
8	209.03		316.41
10	212.12		320.54

Decomposition of NH_4VO_3 in dry air

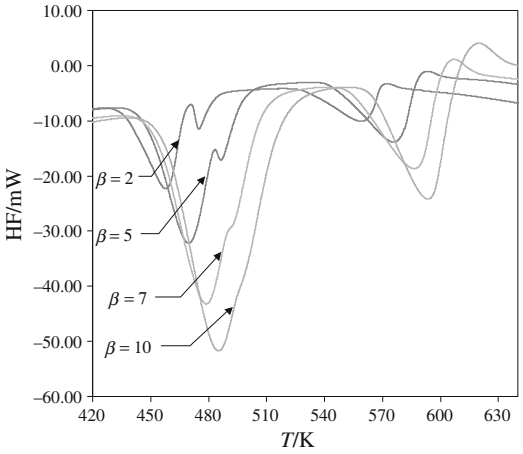

Fig. 6 Plots of HF functions in temperature. Decomposition of NH_4VO_3 in dry air

transition attributed to the oxidation of small amount of V_2O_{5-x} to V_2O_5. Along with the increase of sample heating rate stages I and II overlap. In Table 3 the values of T_m temperatures corresponding to the HF peaks determined for all the series are given.

There should be added that NH_3, H_2O, NO, and N_2O evolved in all the stages, also at higher sample heating rates. In Fig. 7 the results obtained at sample heating rate of 8 K/min are presented as an example.

Analysis of α(*T*) plots for determined stages

The conversion degrees for stages were calculated from the following formula

$$\alpha(T) = \frac{m_0 - m}{m_0 - m_k} \quad (2)$$

where, m_0 is the initial sample mass for the stage/mg, m is the current sample mass for the stage/mg, m_k is the final sample mass after for the stage/mg.

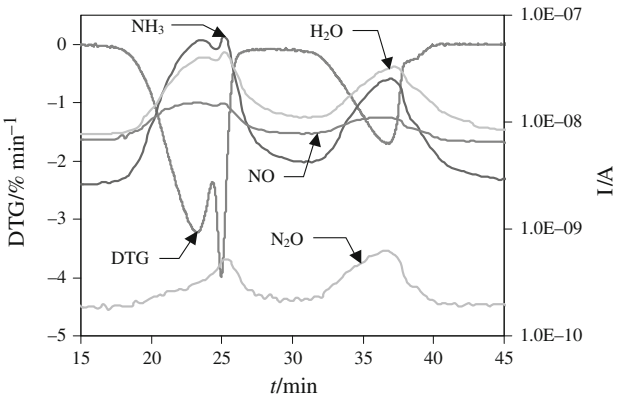

Fig. 7 Functions of DTG and mass spectra of NH_3, H_2O, NO, and N_2O in time. Decomposition of NH_4VO_3 in dry air, $\beta = 8$/K/min

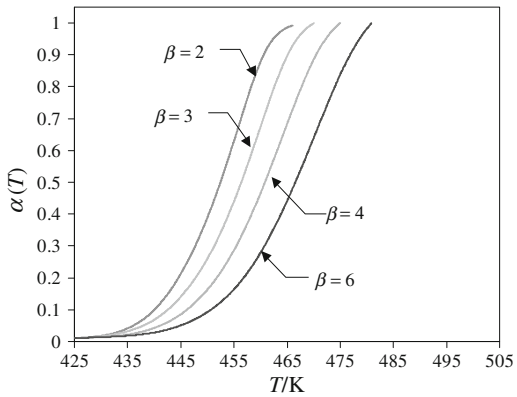

Fig. 8 Dependency of conversion degree on temperature for stage I. Decomposition of NH_4VO_3 in dry air

The data concerning the TG_u function were the basis for calculations. During the division of the process into stages also DTG and HF plots were taken into account.

In Fig. 8 the results obtained for stage I are presented.

The plots of $\alpha(T)$ function, in accordance with the theory of kinetics of non-isothermal heterogeneous processes, are shifted into the higher temperature range.

There should be added that each curve is formed by a few thousands of points.

In Fig. 9 the plots of $\alpha(T)$ function for the stage II are presented. This stage could be distinguished only at lower sample heating rates.

At higher sample heating rates, before the end of the stage III, the small amount of V_2O_{5-x} is formed, which is further oxidized to V_2O_5. After the completion of the process the plots of TG_u and DTG end at the level corresponding to V_2O_5. During the calculations of conversion degrees for this stage, the final mass was assumed as the mass corresponding to V_2O_5. In Fig. 10 $\alpha(T)$ function plots obtained for stage III are presented.

The plots of $\alpha(T)$ for $\beta = 6$ and 8 are not monotonic. This is connected with V_2O_{5-x} formed in small amounts.

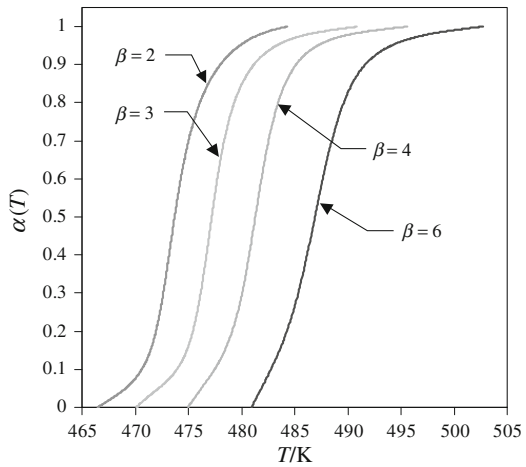

Fig. 9 Dependency of conversion degree on temperature for stage II. Decomposition of NH_4VO_3 in dry air

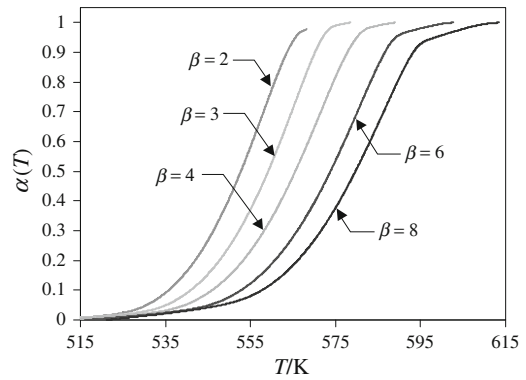

Fig. 10 Dependency of conversion degree on temperature for stage III. Decomposition of NH_4VO_3 in dry air

Conclusions

The results of thermal decomposition of NH_4VO_3 in dry air have been presented. The measurements were carried out by TG–DSC method. The gaseous products were determined by MS method. Solid products were identified by XRD method. On the basis of measurement results the division of the process into stages has been made and the temperature ranges for stage courses and changes of sample masses in stages were determined. There was demonstrated that decomposition of NH_4VO_3 proceeds according to the following equation

$$6NH_4VO_3 \rightarrow (NH_4)_3V_6O_{16} \rightarrow (NH_4)_2V_6O_{16} \rightarrow 3V_2O_5 \quad (3)$$

In all the stages at different sample heating rates NH_3, H_2O, NO, and N_2O were evolved, which were formed as a result of NH_3 oxidation. NO_2 did not occur among the evolved gases. There should be added that N_2O was formed mainly during the stages II and III.

While performing the measurements the emphasis was placed on the possibility of obtaining experimental data for description of kinetics of investigated process, in accordance with ICTAC Kinetics Committee recommendations.

Our observations are following. In case of investigated process the data given for stages, under the isothermal process, could have been obtained only at a few temperatures, but at higher temperatures the results were obtained for higher conversion degrees. In case of non-isothermal measurements with regard to the overlap of stages I and II and formation of V_2O_{5-x} at higher sample heating rates (before end of stage III) the data for needs of iso-kinetic method could be obtained in rather narrow range of sample heating rates ($\beta \leq 4$ K/min).

There should be added that the data for Kissinger method were obtained in slightly larger range of β. For these reasons in this study the results of kinetic calculations concerning the investigated process were not included.

Acknowledgements Financial support of the study by the Ministry of Science and Higher Education within (The National Centre for Research and Development) the project No. NR15-0067-10/2010-2013, is gratefully acknowledged.

References

1. Rogl P, Bittermann H. Ternary metal boron carbides. Int Refract J Hard Mater. 1999;17:27–32.
2. Ye J, Liu Y, Zhao Z, Jiang Z, Tang Z. Synthesis of VC nanopowders by thermal processing of precursor with CaF_2 addition. J Alloy Comp. 2010;496(1–2):278–81.
3. Liu YB, Liu Y, Tang HP, Wang B, Liu B. Reactive sintering mechanism of Ti + Mo_2C and Ti + VC powder compacts. J Mater Sci. 2011;46(4):902–9.
4. Jin Y, Liu Y, Wang Y, Ye J. Synthesis of (Ti, W, Mo, V) (C, N) nonocomposite powder from novel precursors. Int Refract J Hard Mater. 2010;28:541–3.
5. Mutin PH, Popa AF, Vioux A, Delahay G, Coq B. Nonhydrolytic vanadian–titania xerogels: synthesis, characterization, and behavior in the selective catalytic reduction of NO by NH_3. Applied Catal B. 2006;69(1–2):49–57.
6. Debecker DP, Bouchmella K, Delaigle R, Eloy P, Poleunis C, Bertrand P, Gaigneaux EM, Mutin PH. One-step non-hydrolytic sol–gel preparation of efficient V_2O_5–TiO_2 catalysts for VOC total oxidation. Applied Catal B. 2010;94(1–2):38–45.
7. Biedunkiewicz A, Strzelczak A, Możdżeń G, Lelątko J. Non-isothermal oxidation of ceramic nanocomposites using the example of Ti–Si–C–N powder: kinetic analysis method. Acta Mater. 2008;56:3132–45.
8. Biedunkiewicz A, Strzelczak A, Chrościechowska J. Non-isothermal oxidation of TiC_x powder in dry air. Pol J Chem Technol. 2005;7(4):1–10.
9. Biedunkiewicz A, Gordon N, Straszko J, Tamir S. Kinetics of thermal oxidation of titanium carbide and its carbon nano-composites in dry air atmosphere. J Therm Anal Calorim. 2007;88(3):717–22.
10. Coats AW, Redfern JP. Kinetic parameters from thermogravimetric data. Nature. 1964;201:68–9.
11. Vyazovkin S, Wight CA. Model-free and model-fitting approaches to kinetic analysis of isothermal and nonisothermal data. Thermochim Acta. 1999;340–341:53–68.

12. Brauner N, Shacham M. Statistical analysis of linear and non-linear correlation of the Arrhenius equation constants. Chem Eng Proc. 1997;36(3):243–9.
13. Schwaab M, Pinto JC. Optimum reference temperature for reparameterization of the Arrhenius equation. Part 1: problems involving one kinetic constant. Chem Eng Sci. 2007;62(10):2750–64.
14. Sbirrazzuoli N, Vincent L, Vyazovkin S. Comparison of several computational procedures for evaluating the kinetics of thermally stimulated condensed phase reactions. Chemometr Intell Lab Syst. 2000;54(1):53–60.
15. Galway AK. What is meant by the term "variable activation energy" when applied in the kinetic analyses of solid state decompositions (cryptolysis reaction)? Thermochim Acta. 2003;397:249–68.
16. Vyazovkin S, Burnham AK, Criado JM, Perez-Maqueda LA, Popescu C, Sbirrazzuoli N. ICTAC kinetics committee recommendations for performing kinetic computations on thermal analysis data. Thermochim Acta. 2011;520:1–19.
17. Wanjun T, Yuwen L, Xi Y, Cunxin W. Kinetic studies of the calcination of ammonium metavanadate by thermal methods. Ing Eng Chem Res. 2004;43(9):2054–9.